

7C.1 A SIMPLIFIED APPROACH TO UNDERSTANDING BOUNDARY LAYER STRUCTURE IMPACTS ON TROPICAL CYCLONE INTENSITY

Eleanor G. Delap* and Michael M. Bell
Colorado State University, Fort Collins, CO

1. INTRODUCTION

The relationship between tropical cyclone boundary layer (TCBL) structure and tropical cyclone (TC) intensity change is difficult to understand due to limited observations of the complex, non-linear interactions at both the top and bottom boundaries of the TCBL. Consequently, there are debates on: how the TCBL interacts with the mean vortex above, how much surface friction it is interacting with, and how these interactions affect intensity change.

To begin to address these questions, a conceptual framework of how axisymmetric dynamics within the TCBL can impact TC intensity change will be developed from first principles in the form of a new, simple logistic growth equation (LGE). Although this LGE bears some similarities to the operational LGE Model (LGEM; DeMaria 2009), the difference is that our growth-limiting term incorporates TCBL structure and surface drag. The validity of the new LGE will also be explored in idealized numerical modeling and in two observational datasets.

2. DATA

We will use the axisymmetric Cloud Model 1 (CM1) to validate the LGE (Bryan and Fritsch 2002). We will also investigate the existence of LGE relationships in two observational datasets: Hurricane Joaquin (2015) high definition sounding system (HDSS) dropsondes from the Tropical Cyclone Intensity Experiment (Bell et al. 2016; Doyle et al. 2017), and the 2016–2017 Hurricane Research Division (HRD) airborne radar vertical cross-sections.

3. RESULTS AND CONCLUSIONS

3.1 UNDERSTANDING THE LGE

From first principles, we will start with the axisymmetric tangential component of the momentum equation in polar coordinates:

$$\frac{\partial \bar{v}}{\partial t} + \bar{u} \frac{\partial \bar{v}}{\partial r} + \bar{w} \frac{\partial \bar{v}}{\partial z} + \frac{\bar{u}\bar{v}}{r} + f\bar{u} = F_\lambda, \quad (1)$$

where the overbars denote axisymmetric averages; $\frac{\partial \bar{v}}{\partial t}$ is the Eulerian time tendency; $\bar{u} \frac{\partial \bar{v}}{\partial r}$ and $\bar{w} \frac{\partial \bar{v}}{\partial z}$ are the radial and vertical advection of tangential wind, respectively; $\frac{\bar{u}\bar{v}}{r}$ is the centrifugal acceleration; $f\bar{u}$ is the Coriolis acceleration; and F_λ are the nonconservative accelerations.

In a TC, the maximum tangential velocity is typically near the top of the TCBL (Zhang et al. 2011). Therefore, solving at the tangential wind maximum implies solving inside the TCBL. With a few assumptions, the resulting LGE becomes:

$$\frac{\partial \bar{v}_{max}}{\partial t} = \left(-\frac{\bar{u}}{r}\right) \bar{v}_{max} - \left(\frac{\alpha^2 c_D}{z_{ref}}\right) \bar{v}_{max}^2, \quad (2)$$

where the first term on the right-hand side is the growth-rate term, and the second term is the growth-limiting term. We will refer to the ratio of the coefficients as the Instantaneous Logistic Potential Intensity (ILPI):

$$ILPI = \frac{(-\bar{u})z_{ref}}{\alpha^2 r_{max} c_D}. \quad (3)$$

However, while the ILPI is a type of maximum potential intensity (MPI) analogous to a population's "carrying capacity," it is distinct from a *priori* MPI estimates due to its dependence on an existing TC.

Examination of the ILPI yields several results. Most notably, the only way the ILPI can become negative is if there is radial outflow at the tangential wind maximum. However, a negative ILPI is not the only way to decrease \bar{v}_{max} ; it will also decrease if $0 < ILPI < \bar{v}_{max}$ (Fig. 1). In contrast, there are several ways to increase the ILPI: the radial inflow at \bar{v}_{max} can be increased, the height of \bar{v}_{max} can be increased, the vertical gradient of tangential wind can be increased such that α^2 is decreased, the

* Corresponding author address: Eleanor G. Delap, Colorado State University, Dept. of Atmospheric Science, Fort Collins, CO 80523; email: eleanor.delap@colostate.edu

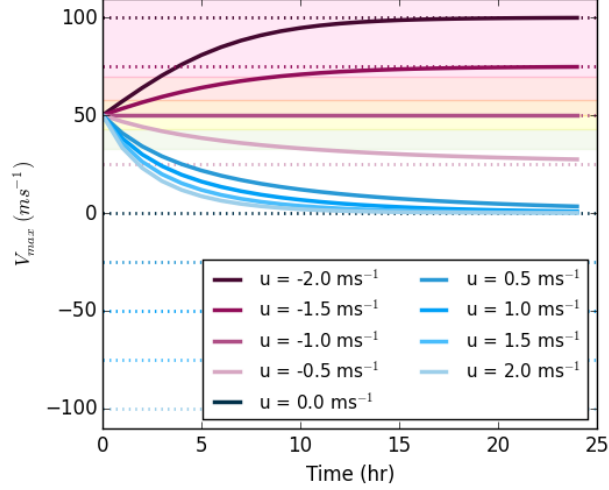


Fig. 1. Arbitrary parameters that illustrate the relationship between the ILPI and \bar{v}_{max} . Shading denotes the Saffir-Simpson scale, dotted lines denote the ILPI, and solid lines denote \bar{v}_{max} for each \bar{u} .

radius of \bar{v}_{max} can be decreased, and c_D below \bar{v}_{max} can be decreased.

By increasing the ILPI farther above \bar{v}_{max} , the intensification rate is also increased due to LGE properties. Thus, a few TCBL parameters can not only provide insight into the sign of TC intensity change, but also its rate of change.

3.2 VALIDATION AND APPLICATIONS OF THE LGE

Modeling and observations show evidence that the relationships seen in the ILPI may be reasonable. Results from CM1 show that the ILPI calculated on hourly timesteps can capture \bar{v}_{max} trends (Fig. 2a). While the ILPI is sensitive to when $\bar{u} \geq 0$, \bar{v}_{max} tends to decrease during these instances and support the relationship. In addition, axisymmetric analyses of Hurricane Joaquin show that the most rapid weakening occurred after \bar{v}_{max} was in radial outflow (not shown). Additional results from the HRD cross-sections may also indicate a direct relationship between \bar{u} and future \bar{v}_{max} . However, more axisymmetric data coverage is needed to fully examine LGE relationships.

Beyond relating TCBL structure to intensity change, a potential application of the LGE is to retrieve c_D from variables that can be measured from research aircraft. Eq. 2 can be solved for c_D such that:

$$c_D = -\frac{\bar{u}z_{ref}}{\alpha^2 r_{max} v_0} \left(\frac{v_0}{\bar{v}_{max}} - e^{\frac{\bar{u}}{r_{max}} t} \right). \quad (4)$$

Results show that while c_D retrievals are noisy, the average is near the CM1 “truth” (Fig. 2b). In addition, when c_D is held constant from 0.0005–0.005, Eq. 4 can generally retrieve c_D to within plus or minus twice the CM1 truth (Fig. 3). However, as the set c_D increases above 0.003, there are noticeably more retrieved negative c_D values due to more frequent instances of $\bar{u} > 0$.

Overall, the simplicity of the LGE aides in the conceptual understanding of the TCBL, and its applications could aide in c_D retrievals and forecasting TC intensity.

Acknowledgements This research is supported by ONR Awards N000141512601 and N000141712230.

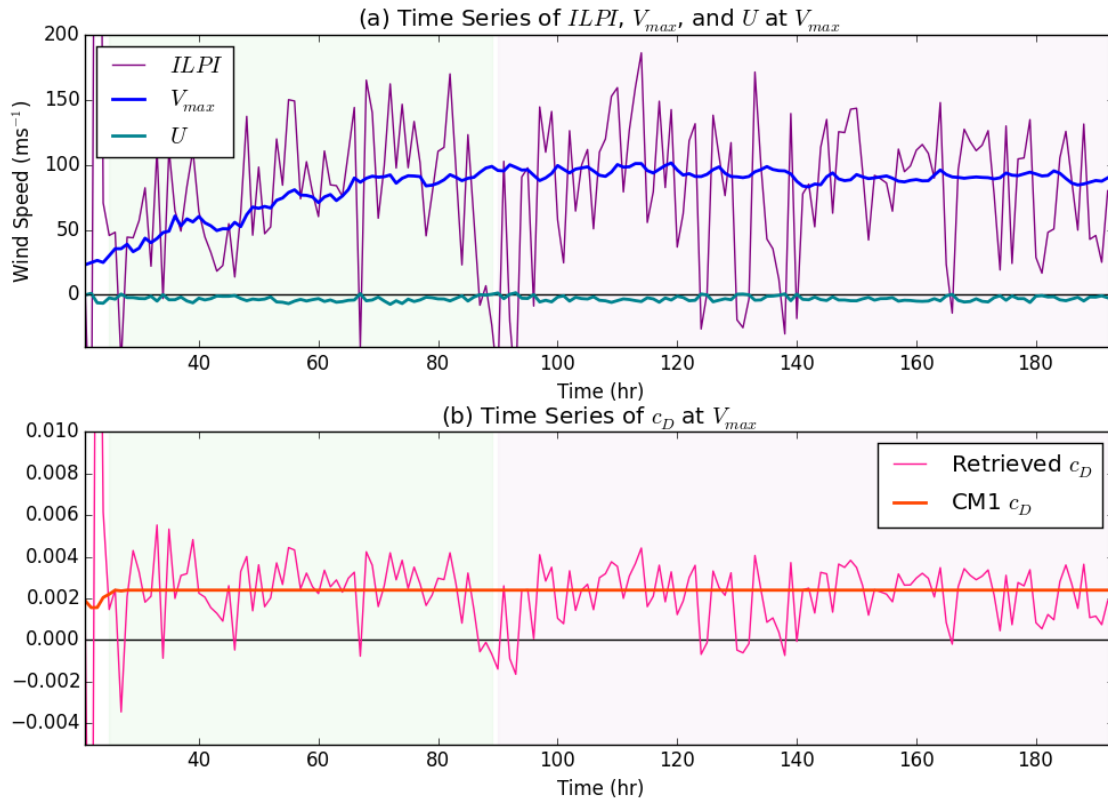


FIG. 2. Time series of: (a) $ILPI$, \bar{v}_{max} , and \bar{u} in ms^{-1} ; and (b) retrieved and CM1 c_D . Green shading denotes increasing \bar{v}_{max} , and purple shading denotes approximately steady-state \bar{v}_{max} .

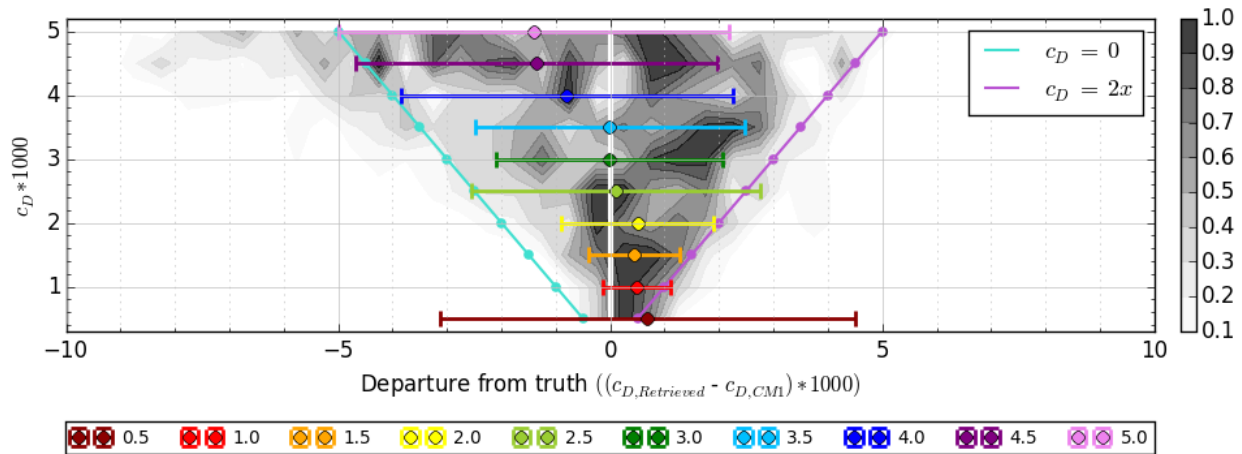


FIG. 3. Shading denotes normalized, vertically-stacked histograms of retrieved c_D anomalies for 10 CM1 simulations with set c_D ranging from 0.0005–0.005. The turquoise line represents when $c_D = 0$, and the purple line is when c_D is twice the set value. Rainbow points and error bars show the anomaly mean and standard deviation of each histogram, respectively.

REFERENCES

- Bell, M. M., and Coauthors, 2016: ONR Tropical Cyclone Intensity 2015 NASA WB-57 HDSS dropsonde data, version 1.1. UCAR/NCAR Earth Observing Laboratory, accessed 23 January 2017, doi: [10.5065/D6KW5D8M](https://doi.org/10.5065/D6KW5D8M).
- Bryan, G. H., and J. M. Fritsch, 2002: A benchmark simulation for moist nonhydrostatic numerical models. *Mon. Wea. Rev.*, **130**, 2917–2928, doi: [10.1175/1520-0493\(2002\)130<2917:ABSFMN>2.0.CO;2](https://doi.org/10.1175/1520-0493(2002)130<2917:ABSFMN>2.0.CO;2).
- DeMaria, M., 2009: A simplified dynamical system for tropical cyclone intensity prediction. *Mon. Wea. Rev.*, **137**, 68–82, doi: [10.1175/2008MWR2513.1](https://doi.org/10.1175/2008MWR2513.1).
- Doyle, J. D., and Coauthors, 2017: A view of tropical cyclones from above: The Tropical Cyclone Intensity experiment. *Bull. Amer. Meteor. Soc.*, **98**, 2113–2134, doi: [10.1175/BAMS-D-16-0055.1](https://doi.org/10.1175/BAMS-D-16-0055.1).
- Zhang, J. A., R. F. Rogers, D. S. Nolan, J. Marks, and D. Frank, 2011: On the characteristic height scales of the hurricane boundary layer. *Mon. Wea. Rev.*, **139**, 2523–2535, doi: [10.1175/MWR-D-10-05017.1](https://doi.org/10.1175/MWR-D-10-05017.1).